

Travertines from the Troll thermal springs, Svalbard

Bjørn Jamtveit, Øyvind Hammer, Carin Andersson, Dag K. Dysthe, Jennifer Heldmann & Marilyn L. Fogel

Jamtveit, B., Hammer, Ø., Andersson, C., Dysthe, D.K., Heldmann, J. & Fogel, M.L.: Travertines from the Troll thermal springs, Svalbard. *Norwegian Journal of Geology*, Vol. 86, pp. 387-395. Trondheim 2006. ISSN 029-196X.

The Troll and Jotun hot springs are located along the Bockfjorden fault zone at 79°23'N on Svalbard and represent the northernmost thermal springs documented on land. They are recharged through subpermafrost aquifers supplied mainly by glacial meltwater and derive their Ca and CO₂ contents from Proterozoic marbles. Gases exsolved from the 25-28°C hot spring waters are N₂ and CO₂-dominated with high contents of He (reaching 1.5% in the Jotun springs) and Ar. The temperature distribution and temporal variation in the main Troll spring have been constrained by IR-photography and by temperature loggers embedded in the springs and associated, water-filled travertine pools over a period of one year. High-resolution micro-drilling techniques have allowed detailed stable isotope profiles to be obtained from selected travertine cross-sections. The data reflect seasonal fluctuations in temperatures during travertine growth and constrain the travertine growth rate. Most of the travertine growth occurs during the summer season as most of the flooded travertine pools were probably frozen for about 6 months per year. Oxygen isotope variations among the travertine terraces partly reflect fluctuations in the spring source composition. These fluctuations have been used to constrain the temporal evolution of the terrace system.

Bjørn Jamtveit (e-mail: bjorn.jamtveit@geo.uio.no), Øyvind Hammer, Dag K. Dysthe, *Physics of Geological Processes (PGP)*, University of Oslo, P.O. Box 1048 Blindern, 0316 Oslo, Norway; Carin Andersson, *Bjerknes Centre for Climate Research*, Allégaten 55, 5007 Bergen, Norway; Jennifer Heldmann, *Jet Propulsion Laboratory*, 4800 Oak Grove Drive Pasadena, California 91109, USA; Marilyn L. Fogel, *Geophysical Laboratory*, Carnegie Institution of Washington, 5251 Broad Branch Rd., N.W, Washington, DC 20015, USA.

Introduction

Travertine deposits normally form when CO₂-rich, Ca-bearing, fluids are exposed to the low pressures at the surface of the Earth. In such cases, calcite precipitation is driven by CO₂-loss and associated pH-reduction during fluid equilibration with the atmosphere (Dreybrodt et al. 1992). Travertines may also occasionally form when extremely basic, Ca(OH)₂-rich fluids absorb CO₂ upon exposure to air.

Travertine deposits are distributed over most of the world (Pentecost 1995) and represent some of the most spectacular examples of self-organized patterns formed at the Earth's surface (Hammer et al. in press; Jettestuen et al. 2006). The travertine patterns include both the external rimstone and terrace-shaped morphologies and the internally layered structure of travertine deposits.

In this contribution we will focus on the travertine deposits located around the Troll springs, located at 79°23'N, 13°26'E near the shore of Bockfjorden on Svalbard (Fig.1). Sampling of spring fluids and travertines were done during three subsequent expeditions to Svalbard in the period 2003-2005.

The Troll springs and the nearby Jotun springs are the northernmost documented hot springs on land and were first described by Hoel and Høltedahl (1911). They are located along a major N-S trending fault-zone separat-

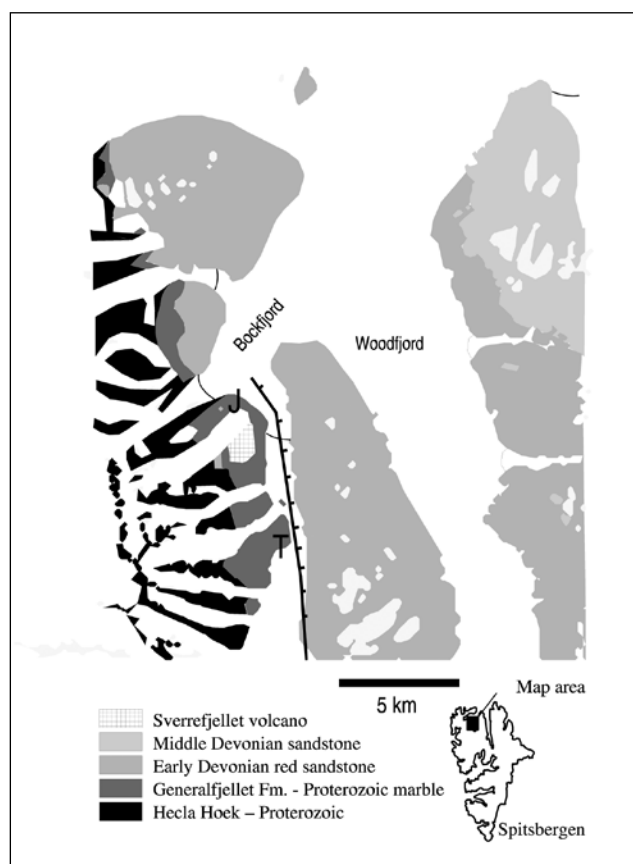


Fig.1: Geological map of the Bockfjorden area, with the locations of the Troll (T) and Jotun (J) springs. White areas on land are glaciers, moraine or sandur.

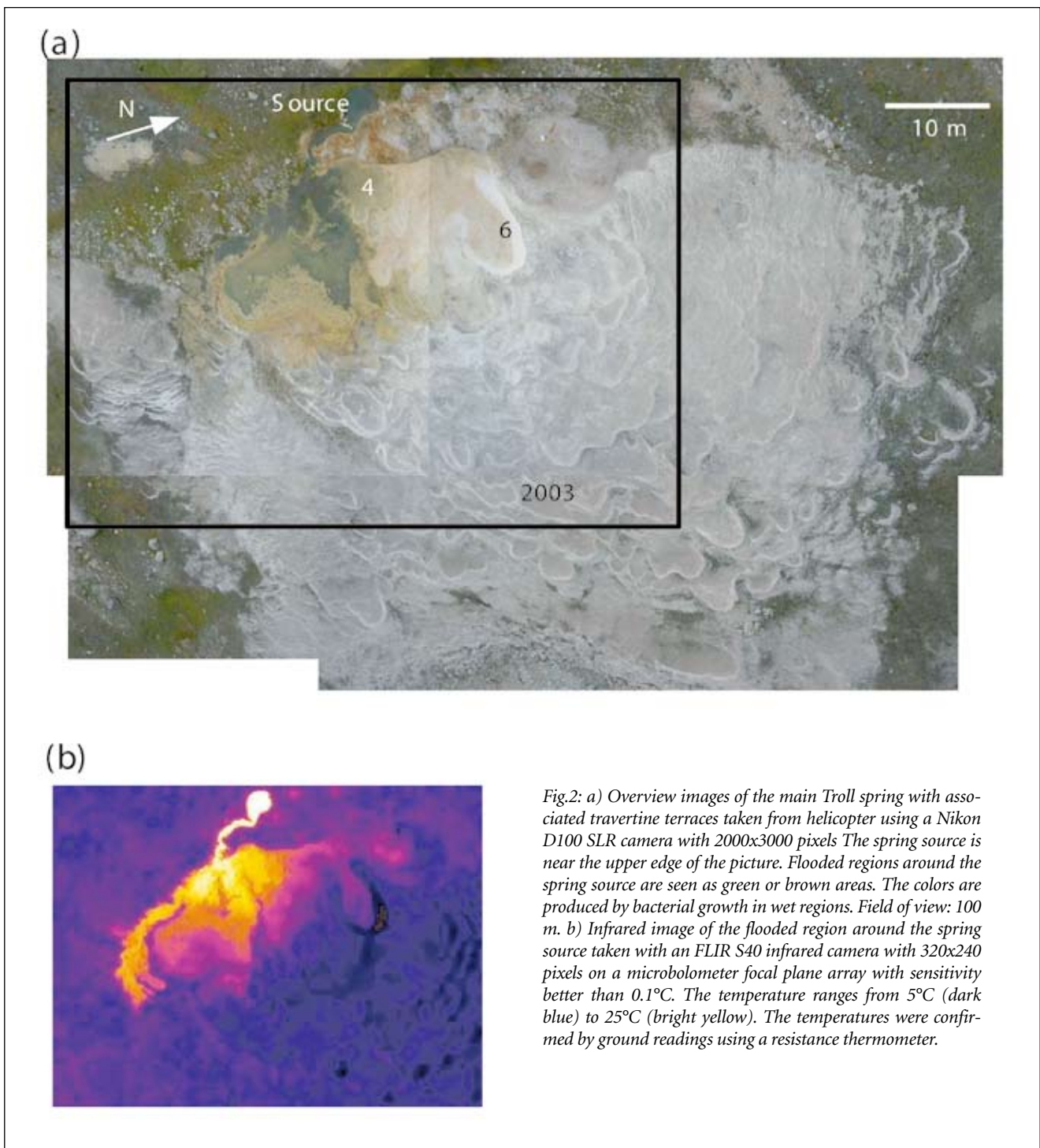


Fig.2: a) Overview images of the main Troll spring with associated travertine terraces taken from helicopter using a Nikon D100 SLR camera with 2000x3000 pixels. The spring source is near the upper edge of the picture. Flooded regions around the spring source are seen as green or brown areas. The colors are produced by bacterial growth in wet regions. Field of view: 100 m. b) Infrared image of the flooded region around the spring source taken with an FLIR S40 infrared camera with 320x240 pixels on a microbolometer focal plane array with sensitivity better than 0.1°C. The temperature ranges from 5°C (dark blue) to 25°C (bright yellow). The temperatures were confirmed by ground readings using a resistance thermometer.

ing Lower Devonian red sandstones from Proterozoic basement rocks. The latter unit includes the Generalfjellet marble formation which represents a likely source of the Troll springs Ca and CO₂ contents. The neighboring Sverrefjell volcano (Fig.1) may have been active as late as in the Pleistocene (Skjelkvåle et al. 1989), but is unlikely to provide thermal energy for the hot spring activity today.

The main travertine terrace system at the Troll locality occurs around the '3A' spring described by Banks et al. (1997). It is around 100 meters across (Fig. 2a), and

only the topmost area is filled with water today. However, pictures taken during the Hoel and Høltedahl expedition (Hoel & Høltedahl 1911) show that a much larger portion of the terrace system has been flooded relatively recently. Thus the flux of water from the 3A spring must have varied significantly over the last 100 years.

The age of the hot spring activity in this area is not known. However, the carbonate structures seen today must have been largely or completely formed after the end of the last glaciation some 8000 years ago, otherwise they would have been eroded away.

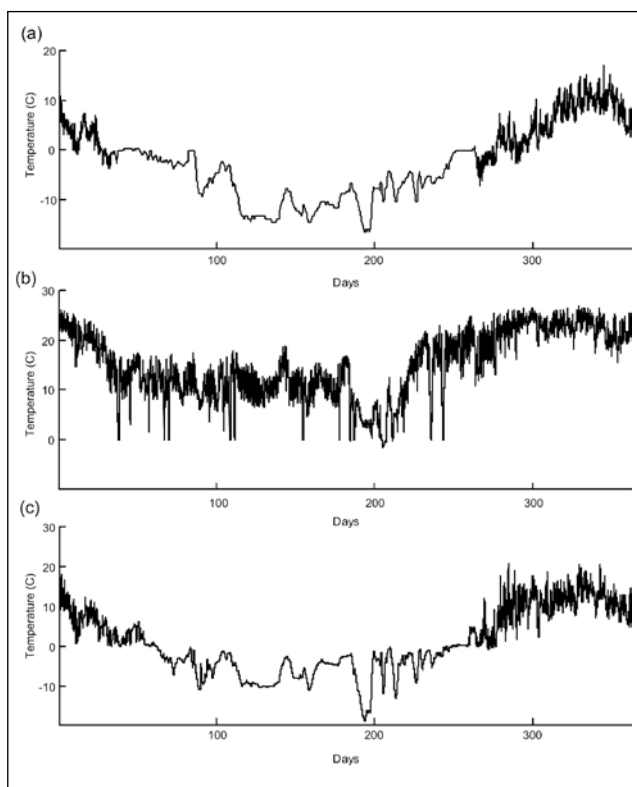


Fig.3: Annual temperature variations in the air and in the springs measured every 30 minutes in the period 14. August 2003 to 15 August 2004. Measurements were done by a HOBO H8 Pro RH/Temperature Logger (air) and a HOBO Stowaway TidBit Logger (water). The reported accuracy is 0.4 °C. a) Air temperature at the Troll springs. Note that the signal gets smoother during the winter season when the temperature logger was covered by snow and temperature fluctuations are dampened. b) Water temperature variations near the spring source (sampling station #4, cf. Fig.2a). c) Water temperature variations further from the spring source (sampling station #6). Again the winter signal is smooth because the distal areas of the ponds freeze and become covered by snow.

Conditions of travertine formation

Temperature fluctuations

The temperatures of the Troll springs are moderate. Hoel and Holtedahl measured a maximum temperature in the source of 28.3°C. We measured source temperatures of the 3A spring to 27.4°C in August 2003 and 25.3°C in August 2005. The temperature distribution and thus the fluid flow paths of the spring waters in August 2005 are clearly visible on an IR-image (Fig. 2b). The image shows that the main flow today is towards the southern part of the terrace system. In 2003 the main flow was towards the northern areas of the flooded pools, but a significant shift in flow path occurred between August 2003 and August 2004. Such shifts are a common feature in the evolution of travertine terrace systems and are at least partly linked to the coupling between the growth of the terraces and the hydro/dynamics of the system (Hammer et al. in press).

Annual temperature variations in the air and in the springs were measured every 30 minutes in the period

14. August 2003 to 15 August 2004, by a HOBO H8 Pro RH/Temperature Logger (air) and a HOBO Stowaway TidBit Logger (water) with an accuracy of about 0.4 °C. Air temperature variations were in the range +16°C to –17°C (Fig. 3a). The average annual air temperature at the Troll springs was –2.5°C. The annual variation in water temperature within the main Troll spring source was not measured, but was likely less than in the neighboring Jotun spring source (with a lower outflow rate) where temperature fluctuations were less than 1.5°C.

Spring water temperatures were measured at two locations in the flooded part of the Troll (3A) spring. The first location (sampling station #4 of Hammer et al. 2005; Fig. 2a) was close to the main source (about 10 meters from the source along the observed fluid flow path), and a second location at the very margin of the flooded region (near sampling station #6; Fig. 2a). At sampling station #4, maximum temperatures were around 25°C in the summer and oscillated around 10°C for most of the winter (Fig. 3b). Temperatures close to freezing were only recorded over brief periods of time. The mean annual temperature was 14.9°C. The temperatures for sampling station #6 were close to air temperatures (Fig. 3c), with an annual mean of 0.6°C and maximum temperatures around 17°C. This distal part of the pools records freezing conditions from mid-October until early May, i.e. for more than 6 months per year. During this period, the travertine pool is covered by ice and snow and little or no travertine growth is possible. Thus, travertine growth rates are expected to show strong seasonal fluctuations.

Spring water composition

The Troll spring water composition was described in detail by Banks et al. (1997) and Hammer et al. (2005). Stable isotope data suggest that the dominant spring water source is sub-permafrost, glacier-derived meteoric waters with a small contribution (ca 1.5 wt%) from waters with seawater-like Br-contents. Cl/Br- and Na/Br-ratios however, depart from seawater and indicate significant fluid/rock interaction effects on Na and Cl contents (Hammer et al. 2005).

From shoreline observations, we know that the sea level has been considerably higher than it is today both during eruption of the Sverrefjell volcano and following the last glaciation. Thus, any seawater-like component in the springs today, is likely to represent 'fossil' seawaters rather than modern 'Bockfjorden-like' waters.

The Troll 3A spring source composition is close to $\delta^{18}\text{O} = -17.5\text{‰}$, $\delta\text{D} = -132\text{‰}$ (relative to the SMOW standards), and $\delta^{13}\text{C} = -1.0\text{‰}$ (relative to PDB). Sub-permafrost groundwater aquifers recharged by glaciers have previously been reported from Western Svalbard by Haldorsen et al. (1996).

As the spring water flows down the terrace system, the

main factors affecting the fluid composition are: CO_2 -loss to the atmosphere, evaporation (H_2O -loss), carbonate-precipitation, and biological activity. Evaporation within the pools that were flooded in 2003 caused downstream shifts (increase) in $\delta^{18}\text{O}$ -values of nearly 1‰ over a distance of ca. 30 meters (along the fluid flow path) due to preferential loss of the light O-isotope during 2-3% evaporation (Hammer et al. 2005).

Temporal variations in the travertine $\delta^{18}\text{O}$ -composition may therefore (in the absence of possible kinetic effects on the carbonate composition) arise due to three different factors: variations in source fluid composition, temperature fluctuations at the site of precipitation, and variable degrees of evaporation.

Gas compositions

Gases emanating both from the Troll and Jotun springs were collected during the 2005 expedition and analyzed by gas chromatography at the Geophysical Laboratory in Washington. The gases are dominated by N_2 (ca 70 vol%) and CO_2 (25-30%), but also contain considerable amounts of noble gasses. CO_2 (gas) C-isotope compositions are about -7‰ for both the Troll and Jotun springs, broadly consistent with C-isotope equilibrium between dissolved carbonate in spring waters (-1‰), exolved CO_2 gas, and travertine carbonates (2-4‰).

The He-contents are exceptionally high in both springs, reaching 1.4% in the Jotun spring and 0.8% in Troll. If this He is of crustal origin, it could be taken as an indi-

cation of very high crustal residence time for the spring waters (eg. Andrews 1983; Giggenbach 1983).

N_2/Ar ratios from the Jotun spring are close to the expected value for air-saturated meteoric waters (ca 40), but is much higher in the Troll springs (ca 200). The excess N_2 in the Troll springs may possibly reflect alteration of organic matter at depth, or contributions from a deeper unknown (magmatic?) source. Both springs furthermore contain a modest amount of methane (0.04 and 0.05%).

Travertine composition

Important clues about the temporal evolution of the travertine-forming system can be obtained by detailed studies of compositional variations within the travertine system. We have carried out oxygen and carbon-isotope analyses both along a profile across an individual layered sample from the central area of the travertine deposit (Figs. 4a), and from samples collected near the surface across the entire terrace system. The travertine profile was also characterized in terms of trace element variation. Finally, we analysed selected surface samples for organic carbon content and the relative variations in organic and inorganic carbon-isotope composition.

Analytical methods

O and C isotope analyses were obtained along a 46 mm

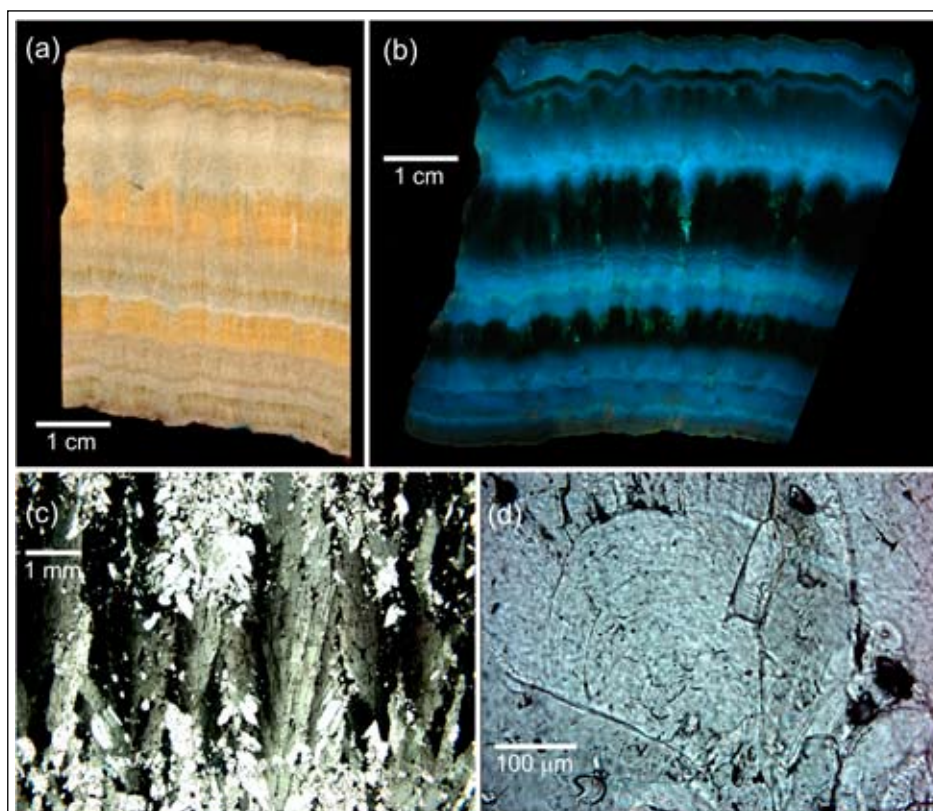


Fig. 4: Travertine structures from sample collected from the steep rim of a travertine terrace at sampling site #2003 (Fig. 2a). a) Cut and polished section of a ca. 5 cm thick sample. The layering is approximately parallel to the outer growth surface. b) Photograph of section of the sample as in a) but taken in 365 nm ultraviolet light using a Suprasil (fused silica) fiber-optic beam with a UV-condensor lens to produce a homogeneous light intensity across the sample surface. c) Microphotograph of large feather-like calcite crystals from the thickest yellowish layer seen in a). d) Possible diurnal layering seen in wedge-shaped calcite crystal. Layer thickness typically on the order of 10mm, corresponding to an annual growth of ca 4 mm.

long profile across the travertine layers of sample #2003 (Figs. 4a and 2a for location of sample). High-resolution sampling was performed using a *Merchantec MicroMill* (New Wave Research). The MicroMill is a micro-sampling system designed for high-precision milling of solid materials. The system comprises a fixed drill with computer controlled sample motion. Using the MicroMills live video image of the specimen, 1 mm long scan lines were sampled parallel to the banding of the travertine specimen. Sub-sampling paths were then interpolated between these scan lines to achieve an approximate spacing of 100 μm between the original sampling paths. The spatial resolution of the milled samples is between 0.098 and 0.109 mm, with an average of 0.103 mm. Each sample was milled to a depth of 0.1 mm and subsequently collected on a glass fiber filter (Whatman GF/F) using a vacuum. The small filters were then transferred to a glass vial for mass spectrometer analysis. The isotope analyses were performed following phosphoric acid extraction (avoiding contamination by organic C) at the Bjerknes Centre for Climate Research at the University of Bergen to a reported analytical precision of about 0.05‰ for C and 0.1‰ for O. Carbonate values are reported relative to the PDB standards.

Travertine samples for analysis of organic C were separated into layers by mechanical breaking and powdering at the Geophysical Laboratory in Washington DC. Typical layers analysed were 2-3 mm thick and showed a range of colors from green and pink to tan, brown and almost black. Green layers were associated with obvious endolithic growth. Pink, white, or brown layers did not have endoliths easily seen by eye. An aliquot (~400 to 1000 μg) of total rock sample was weighed into a tin capsule, which was sealed and introduced into the autosampler (A2100) of a CE Instruments, NA 2500 series EA. Isotope ratios of the combustion gases were analyzed using continuous-flow, stable isotope ratio mass spectrometry (Finnigan MAT, Delta^{plus}XL). For organic carbon isotopic ratios and concentration, ~5 mg of travertine powder were weighed into a hexane-rinsed silver capsule. The carbonates were acidified by adding ultrapure constant boiling, 6 N HCl (100 ml in 20 ml aliquots). The samples were incubated overnight in a fume hood to remove unreacted acid, then dried at 100°C until just before analysis by the methods above. Acetanilide ($\text{C}_8\text{H}_9\text{NO}$) was analyzed to monitor the accuracy and precision of isotopic ratios and elemental compositions by the elemental analyzer. Precision was calculated based on repeat measurements of the same standard: $\delta^{13}\text{C} \pm 0.33\text{‰}$. Carbonates, NBS-19 and NBS-18 were combusted in the EA, and used as internal standards. By this method, $\delta^{13}\text{C}$ values were generally within 0.5‰ of $\delta^{13}\text{C}$ determined by phosphoric acid extraction.

The travertine profile

O- and C-isotope data of carbonate samples collected with high spatial resolution may provide valuable insights into changing conditions during carbonate

growth. A close correlation between seasonal temperature variations and stable isotope profiles across open air carbonate deposits precipitated from cold freshwaters (tufa deposits) was recently demonstrated by Matsuoka et al. (2001) and Kano et al. (2003). This emphasizes the potential of layered carbonate deposits as indicators of climate evolution.

The most well defined travertine banding is found in the coarsely crystalline crust formed on the outer rims of the major terraces (see Guo & Riding 1998, for an outline of travertine lithotype terminology). Figure 4 shows cross-sections and microstructures of travertine sample #2003. More detailed information about the travertine structure can be obtained from an image taken in ultraviolet light (Fig. 4b). Yellowish layers in Fig. 4a, are displayed as layers with low ultraviolet fluorescence and appear dark in Fig. 4b. Figure 4b furthermore illustrates how the individual travertine layers are made up by a number of parallel feather-like 'ray' crystals (cf. Folk et al. 1985). A close-up of these is shown in Fig. 4c. Individual crystals occasionally show micrometer scale layering perpendicular to the growth direction (Fig. 4d). Such layering has previously been related to aragonitic micrite laminae and ascribed to diurnal fluctuations (Folk et al. 1985; Guo & Riding 1992). The layer thickness observed in sample #2003 is typically 10-15 mm. If each layer formed within one day, this would correspond to an annual growth rate of ca. 3.5-5.5 mm/year. This is broadly consistent with measured precipitation rates in the travertine pools reported by Hammer et al. (2005), but less than the average annual growth rate inferred from stable isotope profiles (see below). Detailed scanning electron microscope studies reveal the presence of organic filaments and layers enriched in organic material in the top 2-5 mm of this travertine sample.

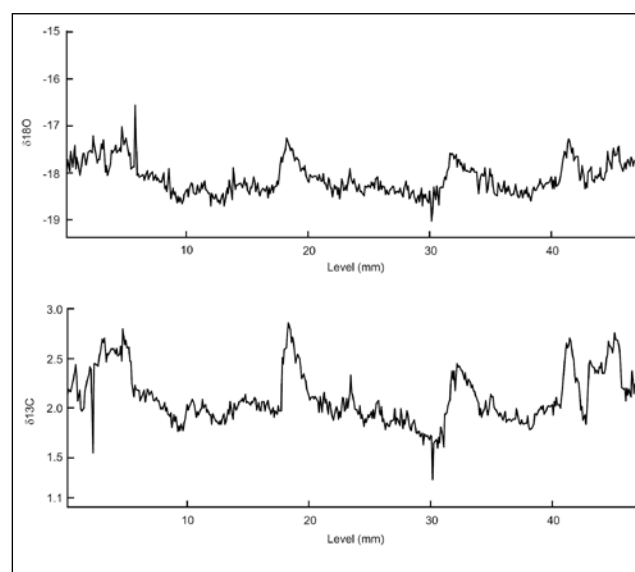


Fig. 5: Oxygen and carbon isotope profiles across travertine sample #2003 obtained by a micro-sampling technique (see main text for technical details). The horizontal scale refers to distance above the lower end of the polished sample shown in Fig. 4a.

Both O and C-isotopes show considerable variations across the profile of sample #2003 (Fig. 5) with a total compositional range of about 1.8‰ and 1.5‰ for O and C respectively. The profiles are characterized by wide regions of light isotope compositions ($\delta^{18}\text{O} = -18.8$ - -18.0 ‰ and $\delta^{13}\text{C} = 1.5$ - 2.1 ‰) separated by narrow peaks where $\delta^{18}\text{O}$ -values approach -17 ‰ and $\delta^{13}\text{C}$ -values approach 2.8 ‰. Autocorrelation diagrams based on any of these profiles show well defined peaks at about 14 mm (Fig.6). This is interpreted as the annual growth rate.

A $\delta^{18}\text{O}$ versus $\delta^{13}\text{C}$ plot (Fig. 7) shows a linear covariation between $\delta^{18}\text{O}$ and $\delta^{13}\text{C}$ for sample #2003. The slope of 1.31 is consistent with temperature fluctuations being the main factor controlling the observed variation (Matsuoka et al. 2001). Thus there is no need for major variations in the spring source composition during the growth period of this 5 cm thick travertine layer.

With temperature as the main source of fluctuations, the zoning patterns observed in Fig.5 can be directly recalculated to a temperature profile provided that the fluid source composition is known and the water-calcite oxygen isotope fractionation is not significantly affected by unknown kinetic effects. To test for isotopic equilibrium, we analysed the isotope composition of carbonate precipitated on the data-logger wire embedded near sample locality #6 of Hammer et al. (2005) during the interval between the field trips in 2003 and 2004. Water samples from this locality were collected both in 2003 and 2005. The compositions were identical within analytical uncertainty (-16.9 ‰). Given the average composition of the carbonate cover on the wire (-16.3 ‰), equilibrium fractionation would indicate an average precipitation temperature of 13.4°C (O'Neill et al. 1969). The water temperatures measured during the 2003 and 2005 field trips were 14.6 and 10.0° . The average water temperature in the period 2003-2004 (i.e. only including temperatures above freezing) was ca. 8.0° . Given the uncertainty regarding possible variations in the carbonate precipitation rate with temperature, these data must be taken as broadly consistent with an equilibrium fractionation model, but do not rule out the possibility of significant kinetic effects on the carbonate isotope composition (cf. Lauritzen & Lundberg 1999).

To check for possible fluctuations in fluid source composition, we analyzed recently precipitated carbonates from the upper water-filled pools (including the carbonate precipitated on wires attached to the temperature loggers) in the period August 2003 to August 2004. These analyses plot on a linear trend parallel to the trend for the #2003 travertine sample (Fig. 7). The slope from recently precipitated carbonate is identical to the slope obtained from the travertine cross-section, but the line is located at about 1.0 ‰ higher $\delta^{18}\text{O}$ -values. This is consistent with the #2003 travertine section being precipitated from a fluid with 1.0 ‰ lower $\delta^{18}\text{O}$ -values than the travertine precipitated today. Assuming that the spring fluid source

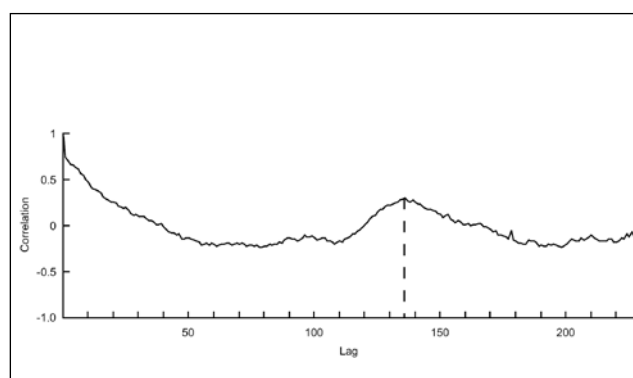


Fig. 6: Autocorrelation of the oxygen isotope profile from Fig. 5. The autocorrelation is the correlation coefficient between the original time series and a time lagged copy, as a function of time lag (e.g. Roberts & Mullis 1987). The autocorrelation peaks at a lag of 137 samples, indicating a periodicity of 13.7 mm.

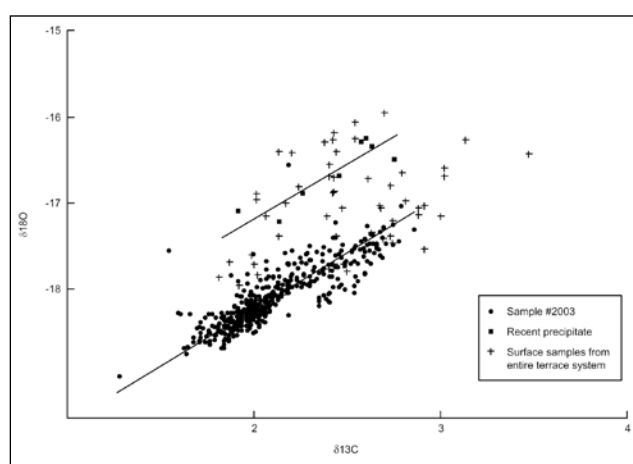


Fig. 7: Oxygen and carbon isotope variation diagram for sample #2003, recent precipitates, and surface samples from the entire terrace system. Regression lines: #2003, $\delta^{13}\text{C} = 1.31\delta^{18}\text{O} - 20.86$, $R^2 = 0.7326$, $N = 449$ (95% bootstrapped confidence interval on slope: [1.237, 1.399]); Recent precipitates: $\delta^{13}\text{C} = 1.31\delta^{18}\text{O} - 19.86$, $R^2 = 0.7822$, $N = 8$ (95% bootstrapped confidence interval on slope: [0.8703, 2.022]);

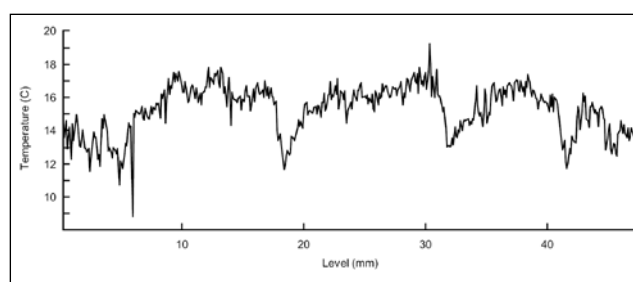


Fig. 8: Temperature fluctuations during growth of travertine sample #2003 calculated from the oxygen isotope profile in Fig.5, assuming that $\delta^{18}\text{O}$ for the local fluid was -18.5 ‰.

composition during precipitation of sample #2003 was -18.5 ‰ (not the current value of -17.5 ‰), the oxygen isotope profile of Fig.5 reflects the temperature evolution shown in Fig.8. There is clearly considerable uncertainty involved in the absolute temperature values in this figure, but the relative variations in temperature should

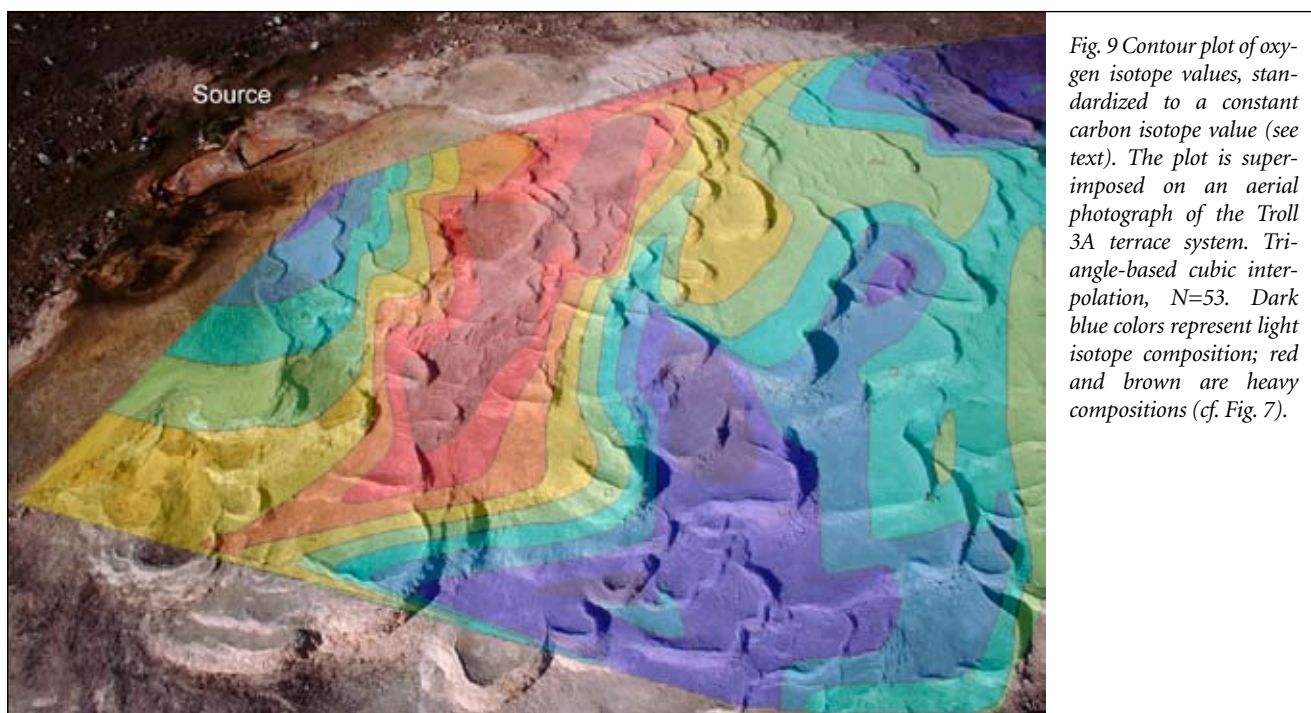


Fig. 9 Contour plot of oxygen isotope values, standardized to a constant carbon isotope value (see text). The plot is superimposed on an aerial photograph of the Troll 3A terrace system. Triangle-based cubic interpolation, $N=53$. Dark blue colors represent light isotope composition; red and brown are heavy compositions (cf. Fig. 7).

be broadly correct. This implies that the broad 'valleys' in the oxygen isotope profile correspond to growth during the summer season when the temperature is highest. The yellow (Fe^{III} -enriched, see below) layers with low ultraviolet fluorescence form in this period. Narrow peaks in the O-isotope profile correspond to growth at lower temperatures. The total temperature range is about 6°C . This is considerably less than the temperature variations obtained in the flooded travertine pools today (Fig. 3), and may reflect higher fluid fluxes and fluid flow rates during the growth of the lower terraces (as suggested by the fact that these pools are dry today). It may also possibly reflect that travertine ceases to grow in the winter season, when the temperature in the pools, at least locally, may have fallen below freezing.

Trace element analyses obtained by electron microprobe reveal that the travertines are very pure CaCO_3 . MgO-contents scatter below 1 wt% and the Fe and Mn contents are generally below 0.05 wt% in terms of FeO and MnO equivalents. There is, however, a significant rise in the Fe-content within the yellow travertine (summer-) layers (Fig. 4a) where Fe-contents rise from less than about 0.05 wt% FeO equivalents in the background, to 0.10-0.15 wt%. The Mg-content is generally very low in the yellow layers, usually less than 0.1 wt%. Ferric iron is well known as an effective inhibitor of fluorescence even at concentrations as low as 0.1 wt% (Waychunas 1988). This is not the case for ferrous iron. We thus conclude that Fe^{3+} (rather than Fe^{2+}) both inhibits the fluorescence in these layers and produces their distinct yellowish color.

Stable isotope variations in the terrace system

The O-, and C-isotope variations between sample #2003 and recently precipitated carbonate suggest that the

spring source composition may fluctuate with time. If this is the case, stable isotope compositional variations within the whole travertine terrace system may provide information about the temporal evolution of terrace system growth. We have therefore analyzed about 60 travertine samples from the whole terrace system with respect to O and C-isotope compositions. All samples were collected from the uppermost carbonate layers found at any given locality, generally $< 1\text{cm}$ from the carbonate surface. Thus, the numbers obtained are representative for the last travertine to precipitate at any given sampling site. Care was taken (by visual inspection) to avoid samples with obvious 'bio-produced' greenish, pink or dark colors.

The results are plotted along with the data for sample #2003 and recent precipitates in Fig. 7. The total range in isotopic composition is $\delta^{18}\text{O} = -18.1$ to -16.0‰ , $\delta^{13}\text{C} = 1.8$ to 3.5‰ . To eliminate variations due to local temperature fluctuations, all data have been recalculated to a constant C-isotope composition by projecting every data-point along a line parallel to the linear trend for sample #2003 (assumed to reflect temperature variations only) until the C-isotope composition is 2.5‰ . Any variation in O-isotope composition following this operation should only reflect variations in fluid source composition or variable degrees of fluid evaporation (H_2O -loss) along the flow path. (This assumes that no spatially systematic variations due to kinetic effects occur).

Figure 9 shows a contour map of the O-isotope compositions across the central terrace system after 'renormalizing' the values to a C-isotope composition of 2.5‰ . As expected, there are significant variations in the O-isotope composition more or less normal to the expected main fluid flow direction. A downstream increase in $\delta^{18}\text{O}$ -val-



Fig. 10 Side-view of the Troll travertine terraces (picture taken from helicopter). Region I and III have 'normal' oxygen 'isotope zonation with increasing values away from the spring source. Region II however, shows decreasing values downslope.

ues is consistent with progressive loss of light isotopes by evaporation. By comparison with data from Hammer et al. (2005), evaporation would typically cause shifts in $\delta^{18}\text{O}$ -values of about +1‰ over 10-30 meters distance along the flow path. Figure 9 clearly demonstrates that this process alone cannot explain the observed isotope variations, which include considerable downstream decreases in $\delta^{18}\text{O}$ -values for parts of the pool system. The most likely explanation for this is temporal variation in the fluid source composition, and thus the data may be used to separate 'generations' of travertine terraces.

Organic C

Green, pink or dark colored samples of the top layers of the travertines typically contain 0.1-0.4 wt% organic C, which represents 1-3% of the total carbon in the samples. Two black and one very green samples showed 6-6.5% C. The organic C composition scatters around -25‰ and typically reduces the total carbon $\delta^{13}\text{C}$ -values by 0.2-0.6‰ compared to the carbonate C composition.

Terrace evolution

Given the spatial resolution of our isotope data (and taking care to avoid samples rich in organic carbon), we can separate three different travertine regions (Fig.10) based on the contours in Fig.9. The upper (I) and lower (III) regions show 'normal' oxygen isotope zoning, in the sense that the isotope values increase away from the fluid source. The gradient is broadly consistent with evaporation being the main controlling factor changing the isotope composition (cf. Hammer et al. 2005). In region II

however, there is a downslope decrease in the $\delta^{18}\text{O}$ -values. If the travertine surface gets younger towards the fluid source region, an explanation may be that variations in the fluid source composition occur. These Change progressively forwards heavier values during precipitation of the travertine found in region II.

This could either reflect changes in the composition of the glacial meltwater source, or the increased effects of fluid rock interactions at depth. The average $\delta^{13}\text{C}$ composition of the travertines is 2.5‰, broadly consistent with the composition of the underlying Generalfjellet marble (three marble samples gave values in the range 1.9-2.3‰). The oxygen isotope composition of the marble is around -9‰ and thus the increasing effects of marble/fluid interactions would tend to produce increasing $\delta^{18}\text{O}$ fluid compositions. Oxygen exchange with silicate rocks would work in the same direction. As the rate of isotope exchange with subsurface rocks is kinetically controlled, the effects would be more pronounced the slower the fluids move through the rocks. Assuming that the reduction of water content in the travertine pools from the Hoel and Holtedahl expedition until today reflects a reduction in fluid flow rate from the spring source, a corresponding increase in $\delta^{18}\text{O}$ -values for the source water is to be expected.

Clearly, the presence of different travertine 'zones' separated by local maxima and minima in the oxygen isotope composition, reflects partial flooding of the travertine terrace system. Complete flooding of the system would have produced a young travertine cover over the entire terrace system with smoothly increasing $\delta^{18}\text{O}$ -values. It is likely that the pattern observed in Fig.9 simply reflects the last stages of terrace evolution when the water has

gradually withdrawn to fill only the pools close to the spring source. Apart from a reduction in fluid flux from the spring source, this may also possibly be affected by increasing leakage of spring fluids from the pools back into the subsurface due to the permeability of the highly porous travertines.

The temporal construction of the full terrace system cannot be constrained by our isotope data as this would require a 3D coverage of travertine samples and thus extensive drilling. Since drilling is forbidden by law in this Arctic nature reserve, quantitative models of the terrace forming processes are constrained by observations from Italian travertine quarries, rather than from the Svalbard travertines (Hammer et al. in press).

Acknowledgements: This study was supported by the Norwegian Research Council by a 'Center of Excellence' grant to PGP. Expedition leader Hans Amundsen (PGP, University of Oslo) and other participants at the 2003-2005 Arctic Mars Analog Svalbard Expeditions ('AMASE') contributed in a major way to this study through discussions and logistic support. UV-images of the travertines were enthusiastically obtained by Jan Kihle (Institute for Energy Technology, Kjeller, Norway) and Muriel Erambert (University of Oslo) conducted trace element analyses of the carbonates by EMP. Constructive reviews by Liane Benning and Stein-Erik Lauritzen significantly improved the manuscript.

References

- Andrews, J.N., 1983: Dissolved radioelements and inert gases in geothermal investigations. *Geothermics* 12, 67-82.
- Banks, D., Siewers, U., Sletten, R.S., Haldorsen, S., Dalen, B., Heim, M., & Swensen, B., 1997: *The thermal springs of Bockfjorden, Svalbard – Hydrogeochemical data report, 97.183*. Geological Survey of Norway, Trondheim.
- Dreybrodt, W., Buhmann, D., Michaelis, J., & Usdowski, E., 1992: Geochemically controlled calcite precipitation by CO₂ outgassing: field measurements of precipitation rates in comparison to theoretical predictions. *Chemical Geology* 97, 285-294.
- Folk, R.L., Chafetz, H.S., & Tiezzi, P.A., 1985: Bizarre forms of depositional and diagenetic calcite in hot spring travertines, central Italy. In N. Schneidermann & P. Harris (Eds.), *Carbonate cements*. Society of Economic Paleontology and Mineralogy, Special Publication 36, 349-369.
- Giggenbach, W.F., Gonfiantini, R., Jangi, B.L., & Truesdell, A.H., 1983: Isotopic and chemical composition of Parbati valley geothermal discharges, northwest Himalaya, India. *Geothermics* 12, 199-222.
- Guo, L., & Riding, R., 1992: Micritic aragonite laminae in hot water travertine crust, Rapolano Terme, Italy. *Sedimentology* 39, 1067-1079.
- Guo, L., & Riding, R., 1998: Hot-spring travertine facies and sequences, Late Pleistocene, Rapolano Terme, Italy. *Sedimentology* 45, 163-180.
- Haldorsen, S., Heim, M., & Lauritzen, S.-E., 1996: Subpermafrost groundwater, Western Svalbard. *Nordic Hydrology* 27, 57-68.
- Hammer, Ø., Dysthe, D.K., & Jamtveit, B., 2006: The dynamics of travertine terrace formation. *Earth and Planetary Science Letters* (in press).
- Hammer, Ø., Jamtveit, B., Benning, L.G., & Dysthe, D.K., 2005: Evolution of fluid chemistry during travertine formation in the Troll thermal springs, Svalbard, Norway. *Geofluids* 5, 140-150.
- Hoel, A., & Holtedahl, O., 1911: Les nappes de lave, les volcans et les sources thermale dans les environs de la baie Wood au Spitsberg. *Videnskapselskapets skrifter (Christiania), I. Matematisk-naturvitenskapelig klasse* 8, 37pp.
- Jettestuen, E., Jamtveit, B., Podladchikov, Y.Y., deVilliers, S., Amundsen, H.E.F., & Meakin, P., 2006: Growth and characterization of complex mineral surfaces. *Earth and Planetary Science Letters* (249, 108-118)
- Kano, A., Matsuoka, J., Kojo, T., & Fujii, H., 2003: Origin of annual laminations in tufa deposits, southwest Japan. *Palaeogeography, Palaeoclimatology, Palaeoecology* 191, 243-262.
- Lauritzen, S.E., and Lundberg, J., 1999: Calibration of speleotherm delta function: an absolute temperature record for the Holocene in northern Norway. *The Holocene* 9, 659-670.
- Matsuoka, J., Kano, A., Oba, T., Watanabe, T., Sakai, S., & Seto, S., 2001. Seasonal variation of stable isotope compositions recorded in a laminated tufa. *Earth and Planetary Science Letters* 192, 31-44
- O'Neil, J.R., Clayton, R.N., & Mayeda, T., 1969: Oxygen isotope fractionation in divalent metal carbonates. *Journal of Chemical Physics* 51, 5547-5558.
- Pentecost, A., 1995: The quaternary travertine deposits of Europa and Asia minor. *Quaternary Science Review* 14, 1005-1028.
- Roberts, R.A. & Mullis, C.T., 1987: *Digital Signal Processing*. Addison-Wesley, Reading, Massachusetts. 578 pp.
- Skjellkvåle, B.L., Amundsen, H.E.F., O'Reilly, S.Y., Griffin, W.L., & Gjelsvik, T., 1989: A primitive alkali basaltic stratovolcano and associated eruptive centers, Northwest Spitsbergen: volcanology and tectonic significance. *Journal of Volcanology and Geothermal Research* 37, 1-9.
- Waychunas, G.A. 1988: Luminescence, X-ray emission and new spectroscopies. In F. C. Hawthorne (Ed.), *Spectroscopic Methods in Mineralogy and Geology*. Mineralogical Society of America, Reviews in Mineralogy, 18.

